Fusion and elastic scattering of $^{9}Be+^{64}Zn$: A search of the breakup influence on these processes

S. B. Moraes, P. R. S. Gomes, J. Lubian,* J. J. S. Alves, R. M. Anjos, M. M. Sant'Anna, I. Padrón,* and C. Muri
Instituto de Física, Universidade Federal Fluminense, Av. Litorânea s/n, Gragoatá , Niterói, R.J., 24210-340, Brazil

R. Liguori Neto and N. Added
Departamento de Física Nuclear, Universidade de São Paulo, Caixa Postal 66318, São Paulo, S.P., 05315-970, Brazil

(Received 1 October 1999; revised manuscript received 10 January 2000; published 12 May 2000)

The role of the breakup process of the weakly bounded light projectile ^{9}Be, on the near barrier fusion reaction and elastic scattering, is investigated by two different approaches. The fusion cross sections for the $^{9}Be+^{64}Zn$ system were compared with the ones from other similar systems (the $^{16}O+^{64}Zn$ and $^{14}N+^{59}Co$). The measurement of the elastic scattering for this system was also used to study the threshold anomaly. There are indications that the fusion suppression due to the ^{9}Be breakup is not important for the interaction of ^{9}Be with this medium mass target.

PACS number(s): 25.60.Bx, 25.60.Pj, 25.60.Gc, 25.70.Mn

I. INTRODUCTION

A subject of recent interest in the field of heavy ion reaction mechanisms at near barrier energies is the investigation of the role of the breakup process of weakly bounded nuclei on the fusion and scattering (reaction) mechanisms. The small separation energies of ^{9}Be (^{9}Be into $^{8}Be+n-S_n=1.67$ MeV or ^{9}Be into $^{5}He+^{4}He-S_\alpha=2.55$ MeV), ^{6}Li (^{6}Li into $^{4}He+^{2}H-S_\alpha=1.48$ MeV), and ^{7}Li (^{7}Li into $^{4}He+^{3}H-S_\alpha=2.45$ MeV) should favor the breakup process, but the consequence of that on other reaction mechanisms is not yet clear. The understanding of the mechanism of the reactions induced by those projectiles should be important for the future understanding of reactions induced by the radioactive ^{11}Li and ^{11} Be beams. The theoretical predictions on this subject are very preliminary and controversial [1–4]. They may predict the enhancement of the fusion due to the coupling of this additional channel [3] or the suppression of the fusion due to the breakup [4]. Also, there are very few experimental data available. Fusion data for light systems ($A_t<25$) [4] show a strong suppression of the fusion for ^{6,7}Li, ^{9}Be induced reactions. For the heavy $^{9}Be+^{208}Pb$ system, an important fusion suppression has also been observed above the Coulomb barrier [5]. In both cases, the suppression of the fusion cross section was explained as a consequence of the absorption of flux by a breakup process.

It is important to study the role of the breakup of those projectiles on different target masses and deformations, in order to investigate the effect, on the fusion, of nuclear and Coulomb breakups and the distance where they occur. In this paper we present and discuss data obtained with the 8UD Pelletron accelerator of the University of São Paulo, for fusion reactions and elastic scattering of the $^{9}Be+^{64}Zn$ system, and we compare the results with the ones obtained by our group for other similar systems $^{16}O+^{64}Zn$ [6,7] and $^{14}N+^{59}Co$ [8,9], where no breakup is supposed to occur.

II. THE FUSION REACTION

A fusion excitation function was measured by the γ-ray spectroscopy method [10]. The bombarding energies were 21, 23, 26, and 29 MeV. The target consisted of metallic ^{64}Zn, with thickness of 496 μg/cm^2, determined by the Rutherford back-scattering method [11] within 5% of uncertainty. A ^{181}Ta backing of 0.12 mm, thick enough to stop the beam, was used to avoid Doppler shifts of the γ lines. The typical beam energy loss on the target was of the order of 0.4 MeV. Two HPGe detectors with Compton suppressors were used, and placed at $\pm55°$ with the beam direction. The detector energy resolutions were 2 keV for the 1332 keV line of ^{60}Co. The efficiency of the detectors was around 30%, and the absolute efficiency was determined by the use of a set of calibrated radioactive sources. Single and coincidence spectra were measured, and the cross sections were determined by the addition of the two single spectra, for each energy. For each bombarding energy, in-beam and off-line decay spectra were accumulated. Care was taken to discount the contribution of the decay of the previous spectra, at each bombarding energy. One backing irradiation spectrum was accumulated, in order to identify the contribution of lines coming from contamination of the target and background. The number of incident particles was determined by the Coulomb excitation of the thick ^{181}Ta backing. All the γ lines of the spectra were identified and, in order to avoid misinterpretation of their origin, the identifications were done not just by their energies, but also by their relative intensities and shape of the excitation functions.

The main limitation of the in-beam γ-ray spectroscopy method for the fusion cross section derivation is the impossibility of identification of the residual nuclei formed directly in their ground state. When the residual nuclei are unstable, with a half-life compatible with the experimental times, the off-beam method is used, and this problem is overtaken. The mentioned limitation, however, is not important for the mass and energy region studied in the present work, as shown in previous works [8,12], where the same evaporation channel cross sections were determined by both γ-ray methods, or the total fusion cross section determination leads to the same

*Permanent address: CEADEN, P.O. Box 6122, Havana, Cuba.

 ©2000 The American Physical Society

TABLE I. Contribution (in %) of each evaporation channel on the fusion cross section and total fusion cross section for the system $^{9}Be+^{64}Zn$.

$E_{c.m.}$	18.2 MeV	19.9 MeV	22.6 MeV	25.2 MeV
σ (mb)	358.3±35	570.1±57	929.7±92	1120.0±112
Channel/E_{lab}	21 MeV	23 MeV	26 MeV	29 MeV
pn	41.4%	36.6%	29.1%	21.3%
$2pn$	1.7%	3.2%	9.9%	18.1%
$2pn+\alpha 2pn$	8.4%	14.3%	28.5%	25.2%
α	0.2%	0.6%	0.5%	0.7%
αp	10.3%	11.4%	4.2%	8.9%
$\alpha 2n$	0.1%	0.2%	0.4%	0.8%
αn	27.9%	25.3%	20.4%	15.3%
$\alpha 2p$	1.4%	1.0%	0.8%	1.2%
$p3n$	4.9%	3.6%	3.1%	2.7%
αpn	0.9%	0.8%	2.2%	4.5%
2α	2.5%	3.0%	1.2%	1.4%

values, when measured by γ rays or particle detection [13].

The uncertainties in the values of the fusion cross sections come from statistical errors in the determination of the γ yields, from systematic errors due to target thickness, absolute efficiency of the detectors, thick target calculation for Coulomb excitation, and errors from the contaminant corrections. The overall cross section error range is from 10 to 15 %.

The total fusion cross sections were obtained by adding the cross sections of each evaporation channel: pn, $p2n$, $2pn$, $\alpha 2pn$, α, αp, $\alpha 2n$, αn, $\alpha 2p$, αpn, 2α. Table I shows the total complete fusion cross sections. For this system the fission channel has negligible cross section. The experimental evaporation cross sections were compared with statistical model predictions, by using the code PACE

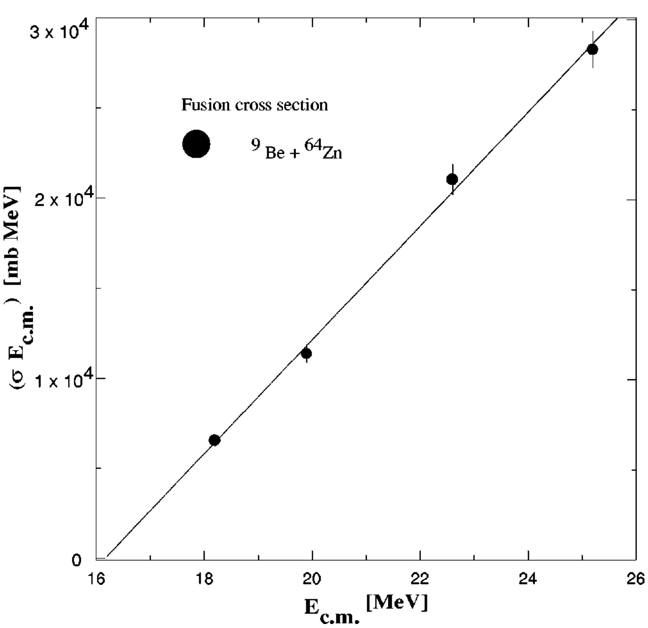

FIG. 1. Fusion excitation function for experimental determination of barrier parameters.

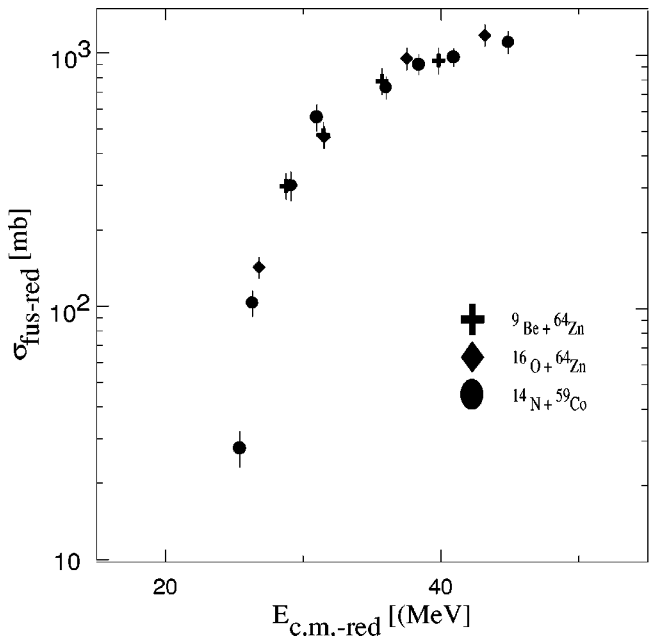

FIG. 2. Comparison of reduced fusion cross section for different systems, where $\sigma_{\text{fus-red}}=\sigma_{\text{fus}}(R_{B,\text{ref}}/R_B)^2$ and $E_{\text{c.m.-red}}=E_{\text{c.m.}}(V_{B,\text{ref}}/V_B)$, and the subscript *ref* means the reference system (taken as the $^{14}N+^{59}Co$ system in this case). The values of R_B and V_B, for the systems not studied in this work, were taken from Refs. [6–9].

[14], and the agreement was quite reasonable for most channels, including the most important ones. In the calculations, the default $A/8$ level density was used, where A is the mass number of the compound nucleus.

From the fusion cross sections, the barrier parameters were derived (see Fig. 1) as $R_B=10.0$ fm (barrier radius) and $V_B=16.2$ MeV (Coulomb barrier), which are within the systematics of Vaz and Alexander [15], and in agreement with the Krappe-Nix-Sierk (KNS) [16] model. The usual way to compare the fusion excitation functions of different systems is to plot the reduced cross sections and the reduced center-of-mass energies (see Refs. [17,18], for example). The reduced fusion cross section, used in order to eliminate geometrical factors for the different systems, is defined as

$$\sigma_{\text{red}}=\sigma\left(\frac{R_{B,\text{ref}}}{R_B}\right)^2, \quad (1)$$

and the reduced center-of-mass energy, used in order take into account the different Coulomb barriers for the systems, is defined as

$$E_{\text{c.m., red}}=E_{\text{c.m.}}\frac{V_{B,\text{ref}}}{V_B}. \quad (2)$$

Figure 2 shows the reduced fusion excitation functions for three systems: $^{9}Be+^{64}Zn$, $^{16}O+^{64}Zn$, and $^{14}N+^{59}Co$, where the $^{14}N+^{59}Co$ system was taken as the reference one. In the $^{9}Be+^{64}Zn$ system, there might be the influence of the ^{9}Be breakup on the fusion process, producing an inhibition of this process. In the $^{16}O+^{64}Zn$ system, with the same target, the projectile is a strongly bounded double magic nucleus. In the ^{14}N+^{59}Co, the same compound nucleus as the ^{9}Be+^{64}Zn is formed.

One can notice that there is no fusion suppression for the ^{9}Be induced reaction, in comparison with the other systems. Moreover, as the barrier parameters derived from the data for the three systems [7,8] are similar to those predicted by the systematics [15] and by a one-dimensional potential model [16], a possible influence of the breakup process on the scaling factors defined in Eqs. (1) and (2) is disregarded. Therefore, there is an indication that the ^{9}Be breakup does not play a major role in the fusion process for this system.

However, one should keep in mind that there might be the contribution of incomplete fusion, following the breakup of the ^{9}Be into $\alpha+\alpha+n$ or ^{9}Be into $\alpha+{}^{5}$He, on the derived fusion cross section. The reason is that the γ rays emitted by the deexcitation of the incomplete fusion residual nucleus, formed through the x channel would be the same as the ones emitted by the deexcitation of the complete fusion residual nuclei formed through the αnx channel. Therefore, what was measured might be the addition of complete and incomplete fusion.

The complete fusion evaporation channels which could possibly be contaminated by the breakup are the αpn, $\alpha 2n$, and $\alpha 2pn$. Figures 3(a), 3(b), and 3(c) show the PACE predictions for these channels and the experimental results. For the αpn and $\alpha 2n$ channels, at high energies, the agreement is reasonable. For the lower energies, the experimental values are higher than the predictions, indicating that there might be some contamination. However, if one notices that the contribution of these channels for the total complete fusion cross section, at these energies, are small (roughly 3 and 0.2 %, respectively), one could neglect this possible contamination. The $\alpha 2pn$ cross section was determined together with the $2pn$ cross section, but the overall agreement is also reasonable.

III. THE ELASTIC SCATTERING

Another approach to study the influence of the breakup on other reaction mechanisms is through the detailed analysis of elastic and inelastic scattering, at near barrier energies. Two pairs of systems have been reported so far: ^{6,7}Li+^{208}Pb [19] and ^{6,7}Li+^{138}Ba [20]. The role of the breakup process on the elastic scattering process is investigated by the analysis of the behavior of the energy dependence of the real and imaginary parts of the optical potentials. A dispersion relation [21,22] associates a peak in the strength of the real part of the optical potential V in the vicinity of the Coulomb barrier, with the decrease of the imaginary part of the potential W as the bombarding energy decreases towards the barrier energy. This behavior is called threshold anomaly. When the coupling of the inelastic and eventual strong direct reaction channels are taken into account, the anomaly is destroyed. The presence of the anomaly can, therefore, be interpreted as the effect of the strong coupling of the elastic channel with the inelastic and direct reaction channels at near barrier energies. Consequently, it may also be interpreted as a signature of the fusion cross section enhancement. It has been reported [23,24], that the coupling to the breakup channel may contribute as a repulsive polarization potential. This repulsive potential may exceed the attractive term arising from the inelastic coupling to the bound states or other direct reaction channels, if there is any relevant coupling, or may be of the same order of magnitude. If there are not any other important reaction channels out of breakup, this might mean that the polarization potential produced by the breakup varies slowly with energy.

From the elastic scattering data, one can also derive the total reaction cross section and compare it with the fusion cross section. Therefore, from the simultaneous study of the fusion excitation functions and elastic scattering angular distributions, one should be able to extract enough information on the fusion and reaction cross sections and polarization potential, in order to contribute to the understanding of the role of the breakup on the fusion, reaction, and scattering processes.

The elastic scattering experiments were also performed at the 8UD Pelletron accelerator of the University of São Paulo. The beam energies were 17, 19, 21, 23, 26, and 28 MeV, corresponding to energies from the nominal Coulomb barrier to 50% above this value. The metallic Zn target had thickness of the order of 50 μg/cm^{2}. The Zn target and one Au target were placed at the target holder at the center of a multipurpose scattering chamber, with a diameter of 1 m. The detection system was an array containing nine silicon surface barrier detectors. The angular separation between two adjacent detectors was 5°. In front of each detector there was a set of collimators and circular slits for the definition of solid angles and to avoid slit-scattered particles. The angle determination was made by a reading on a goniometer with a precision of $\pm 0.5°$. The angular distribution data were taken in the range $25° \leqslant \Theta_{lab} \leqslant 165°$, for the lower energies and up to 95° at the highest one. A monitor was placed at 35° with the beam direction. The relative solid angles of the detectors were determined by the Rutherford scattering of ^{9}Be on the ^{197}Au target. The energy resolutions of the detectors were of the order of 300–500 keV(FWHM). The inelastic peak of the ^{64}Zn was well resolved from the elastic peak. The uncertainties in the differential elastic cross section data vary from 1 to 10 %.

The analysis of the angular distributions was performed by the ECIS code [25]. The real and volume imaginary potentials were of the Woods-Saxon form.

An alternative approach to the elastic scattering analysis is to use the double-folded potential for the real part with the nucleon-nucleon interaction of M3Y kind (see, for example, Ref. [19], and references therein) and the imaginary part of the Woods-Saxon form. One characteristic of these kinds of studies is the need to renormalize the double-folded potential at near barrier energies, as a consequence of the coupling to the breakup channel, where it is relevant (reactions with the ^{6}Li projectile, for example).

It has been shown by Keeley *et al.* [19], studying the elastic scattering of ^{6,7}Li from ^{208}Pb, that the doubled-folding real potential must be normalized for the ^{6}Li +^{208}Pb system by a coefficient around 0.6, at near barrier energies, in order to fit the experimental angular distribu-

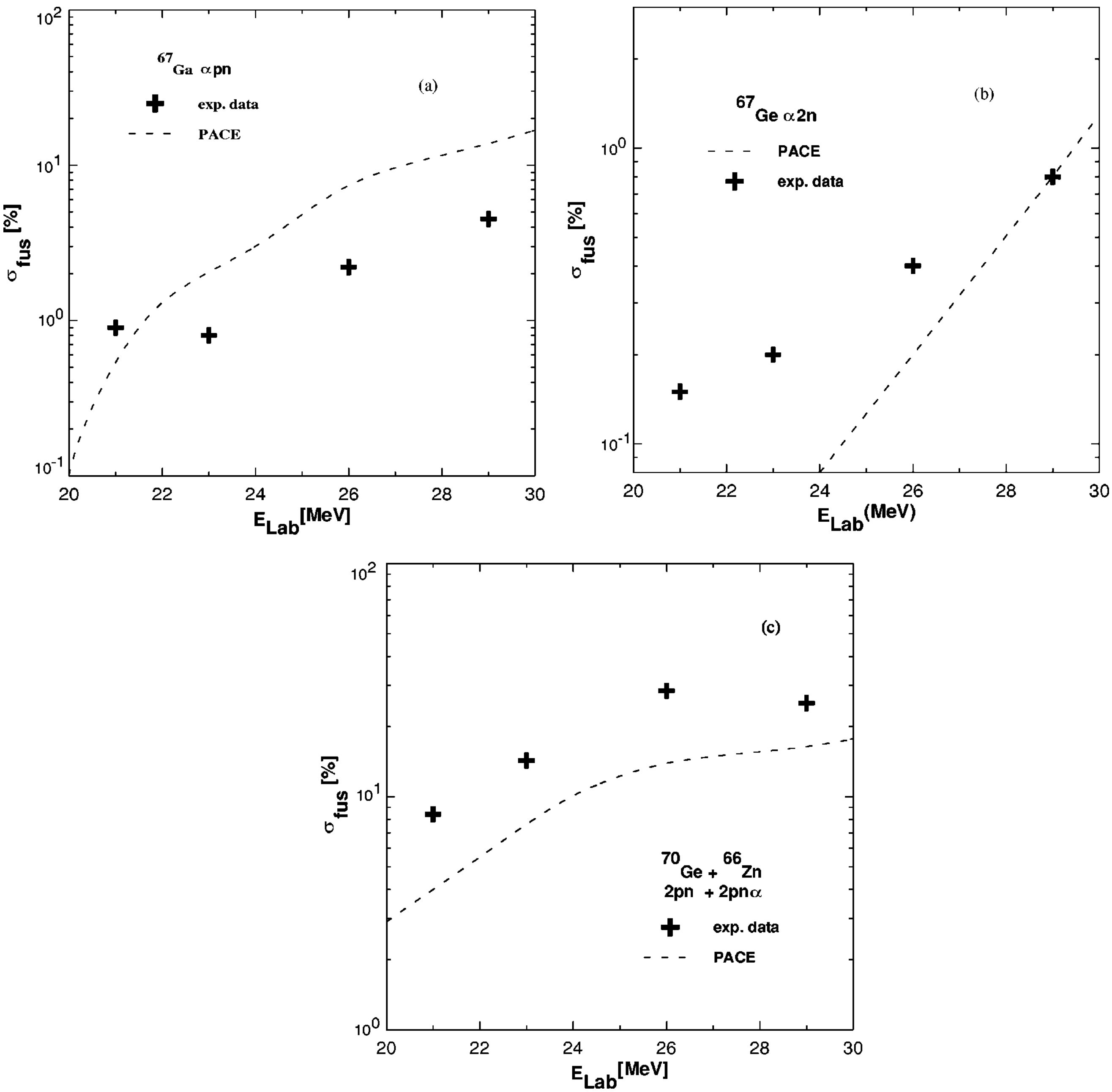

FIG. 3. (a) Comparison between experimental data of percent contribution of αpn evaporation channel to fusion cross section and theoretical PACE predictions. (b) Comparison between experimental data of percent contribution of $\alpha 2pn$ evaporation channel to fusion cross section and theoretical PACE predictions. (c) Comparison between experimental data of percent contribution of $2pn\alpha+2pn$ evaporation channels to fusion cross section and theoretical PACE predictions.

tions. They concluded that the polarization potential produced by the coupling of the breakup channel has a repulsive character, on the basis of the already mentioned studies carried out by Sakuragi *et al.* [23]. Sakuragi and co-workers performed a microscopic calculation of the dynamic polarization potential produced by the coupling of the breakup channel to the elastic channel for the ^{6}Li+^{28}Si, ^{40}Ca at energies well above the Coulomb barrier. In order to extract this polarization potential, they used the coupled discretized continuum channel method [26–28], including the resonance and nonresonance states, and they described the totally antisymmetrized wave function of ^{6}Li on the basis of the α-d cluster model. They showed that the real part of the dynamic polarization potential is strongly repulsive, and that its imaginary part has a negligibly small value (nuclear breakup). Then, it was demonstrated that the origin of the strong reduction of the normalization factor for the real potential, required in the double-folding model, is due to the ^{6}Li breakup effect on the elastic scattering.

On the other hand, the study of Keeley *et al.* showed no need for the introduction of this reduction factor for the ^{7}Li+^{208}Pb system, which means that the ^{7}Li breakup is not an important coupling channel. They obtained a potential with the well known anomalous energy dependence, at

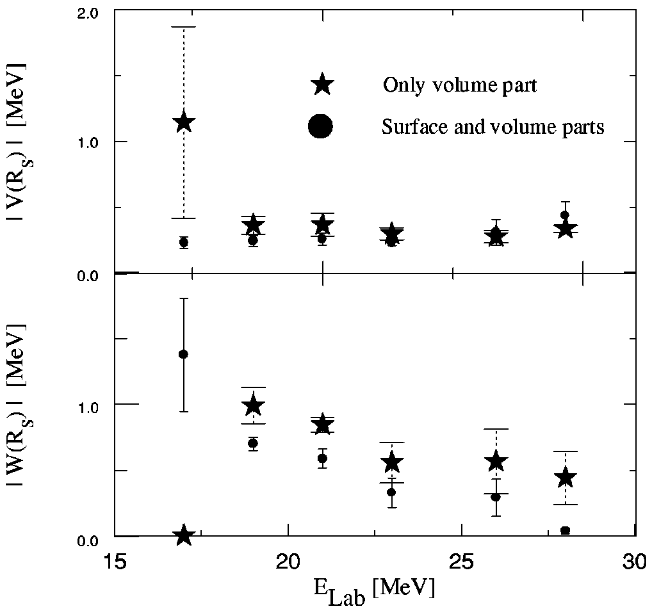

FIG. 4. Energy dependence of the real and imaginary parts of the optical potential at the radius of sensitivity ($R_s = 10.5$ fm) for both variants of optical potentials (see text for details).

near barrier energies, for ^{7}Li+^{208}Pb system and no anomalous dependence for the ^{6}Li+^{208}Pb system.

In our previous study on ^{6,7}Li+^{138}Ba [20], using the Woods-Saxon optical potential, the same results as Keeley *et al.* were obtained, i.e., the optical potential anomaly was obtained for the system involving the ^{7}Li as a projectile and no potential anomaly for the system involving the ^{6}Li projectile. Therefore, for very weakly bound nuclei, as the ^{6}Li,

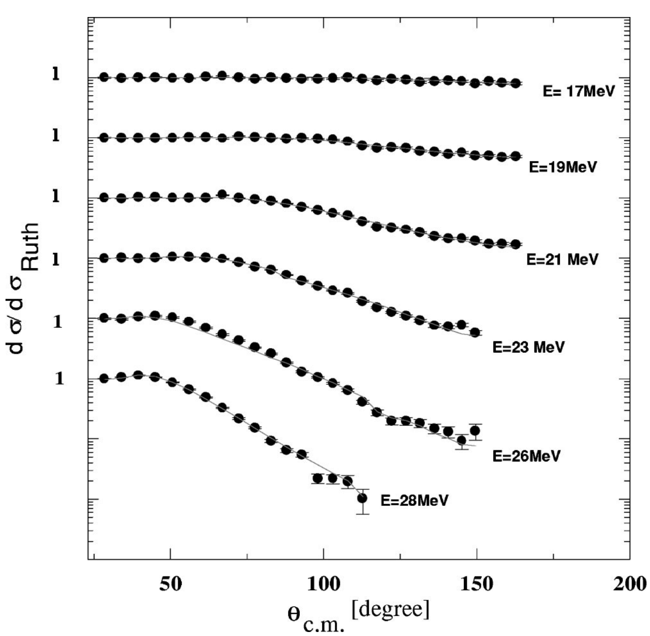

FIG. 5. Elastic angular distribution for the studied energies. The full lines represent the fits with volume and surface imaginary potentials, and the dashed lines represent the fits with volume imaginary potential only. The difference between them is hardly seen.

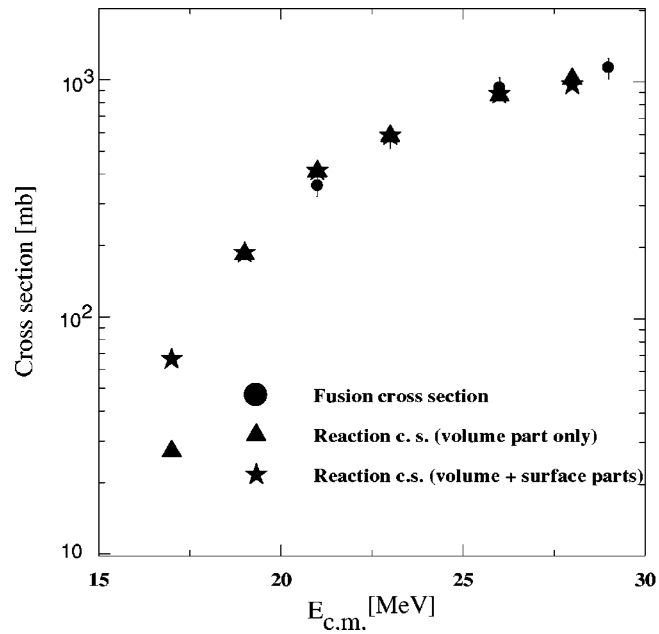

FIG. 6. Comparison of the experimental fusion cross section (full circles) with the reaction cross sections derived from optical model analyses. The full stars correspond to the calculations with volume and surface parts of the imaginary optical potential, and the full triangles, with the volume part only.

the coupling to the breakup channel may be strong enough to affect the real part of the optical potential near the Coulomb barrier in such a way that it leads to the absence of the threshold anomaly in the scattering of these projectiles. On the other hand, for the reactions induced by ^{7}Li on heavy targets, other direct reaction channels, such as the excitation of its first low-lying state, or one neutron transfer reaction [29] may be responsible for the presence of the threshold anomaly at near barrier energies, and the breakup does not play an important role for these systems. From these analyses, there are strong signatures that when the breakup appears to be the most relevant reaction channel, the overall polarization potential varies slowly with the energy.

On the basis of these previous works, the same kind of study, the investigation of the potential anomaly at near barrier energies, using the Woods-Saxon optical potential, was performed for the ^{9}Be+^{64}Zn system.

As we used the Woods-Saxon form factor for the real part of the optical potential, their parameters are owned by the well-known ambiguities [30]. In order to minimize these optical potential ambiguities, one has to find the values of the potentials at the sensitivity radius, found as the position where the different families of optical potential parameters provide the same value of the potential, for a given energy, and providing a good fit of the elastic angular distributions, i.e., the same χ^2. The details of this procedure have been explained in detail in Refs. [9,20,31]. We fixed the reduced radii of the real and the imaginary parts of the optical potentials and varied the diffuseness parameters from 0.5 to 0.8, fm in steps of 0.05 fm, and fitted the angular distributions in order to find the potential strengths.

Figure 4 shows the values of the real and imaginary parts of the optical potential at the radius of sensitivity, for two different variants of sets of optical potential. The first one, full stars, corresponds to the calculations with imaginary volume and surface optical potentials with 1.1 and 1.25 fm for the reduced radii, respectively. The second one, full circles, corresponds to the calculation with only a volume shape for the imaginary part of the optical potential, having a reduced radius 1.25 fm. The choice of this reduced radius for the second variant does not have the usual physical meaning adopted for the volume part of the imaginary optical potential in heavy-ion reactions at near barrier energies, i.e., contribution of the flux to fusion. In this case, it must account for the total absorption of flux from the elastic channel. In both sets, the reduced radius of the real part of the optical potential was of 1.25 fm. One can see from this figure that the two variants have different behaviors for low energies. The calculation with only the volume part of the optical potential shows a drop of the imaginary part for lowest energy and the increment of the strength of the real part. This fact, as mentioned above, and explained in details for the elastic scattering of ^{6,7}Li on ^{138}Ba in Ref. [20], would allow us to say that the breakup channel has no significant effect on the elastic scattering for this system and that the enhancement of the fusion cross section must be produced by the coupling to the inelastic excitations of the low-lying states of the target ^{64}Zn or the one neutron transfer, followed by the decay of the unstable residual nucleus ^{8}Be or another reaction channel. On the other hand, the results with both parts of the imaginary optical potential show almost no anomalous energy dependence, and following the results with the ^{6}Li projectile, could lead us to say exactly the opposite, i.e., that the breakup channel might be the main one responsible for the absence of the threshold anomaly. Both assumptions for the imaginary part of the optical potential give very good fits of elastic angular distributions for this system, as can be seen in Fig. 5. The only important difference between the two sets of the optical potential is the value of the reaction cross section for 17 MeV, that is of 27.2 mb in the case of the only volume part, and 66.5 mb when both volume and surface parts of the imaginary optical potential are included. The study of the reaction cross section versus the inverse of energy showed the well known linear dependence, with a small deviation of this rule for the near barrier energies, in both cases, with reasonable values for the reaction cross section.

Figure 6 shows a comparison between the fusion cross sections and the total reaction cross section, derived from the elastic scattering data. One can see that they are quite similar in the whole energy range where the fusion was measured, leaving no room for a significant cross section for any other reaction mechanism, including the breakup. This is a strong indication that there is no fusion suppression for this system.

IV. CONCLUSIONS

This paper is concerned with the study of the role of the breakup of weakly bound projectile ^{9}Be on the fusion and elastic scattering by medium mass target ^{64}Zn, at energies close to the Coulomb barrier. Fusion and elastic scattering data of ^{9}Be$+^{64}$Zn are presented.

The analysis of the elastic scattering data was not conclusive about the presence of the threshold anomaly. It will be important to measure the fusion cross section (the most relevant channel in the reaction cross section at energies below and near the barrier), at the barrier energy, in order to assess the influence of the breakup channel on the elastic scattering. The simultaneous analysis of the fusion and elastic scattering data at low energies would clarify on the presence or not of the threshold anomaly for this system.

On the other hand, the high-energy fusion cross section results show a strong signature that the fusion is not suppressed by the ^{9}Be breakup. The reason for that might be that the Coulomb breakup plays a major role in the reactions with heavy targets [5], by suppressing the fusion at energies above the Coulomb barrier, but for lighter systems, when the nuclear breakup is predominant and occurs at short distances, the fusion suppression effect is not important. For very light systems, the observed small ratio fusion-reaction cross section [4] might be due to competition with other direct reaction channels, such as transfer reactions, and not necessarily the breakup.

ACKNOWLEDGMENTS

The authors would like to thank the CNPq, FAPERJ, and the CAPES for their partial financial support.

[1] N. Takigawa, M. Kuratani, and H. Sagawa, Phys. Rev. C **47**, R2470 (1993).

[2] M. Hussein, M. P. Pato, L. F. Canto, and R. Donangelo, Phys. Rev. C **46**, 377 (1992).

[3] C. H. Dasso and A. Vitturi, Phys. Rev. C **50**, R12 (1994).

[4] J. Takahashi, M. Munhoz, E. M. Szanto, N. Carlin, N. Added, A. A. P. Suaide, M. M. de Moura, R. Liguori Neto, and A. Sazanto de Toledo, Phys. Rev. Lett. **78**, 30 (1997).

[5] M. Dasgupta, D. J. Hinde, R. D. Butt, R. M. Anjos, A. C. Berriman, N. Carlin, P. R. S. Gomes, C. R. Morton, A. S. Toledo, and K. Hagino, Phys. Rev. Lett. **82**, 1395 (1999).

[6] C. Tenreiro, J. C. Acquadro, P. A. B. Freitas, R. Liguori Neto, G. Ramirez, N. Cuevas, P. R. S. Gomes, R. Cabezas, R. M. Anjos, and J. Copnell, Phys. Rev. C **53**, 2870 (1996).

[7] C. Tenreiro, J. C. Acquadro, P. A. B. Freitas, R. Liguori Neto, G. Ramirez, N. Cuevas, P. R. S. Gomes, and J. Copnell, Proceedings of the Workshop on Heavy Ion Fusion: Exploring the Variety of Nuclear Properties, Padova, Italy, 1994 (unpublished).

[8] P. R. S. Gomes, T. J. P. Penna, E. F. Chagas, R. Liguori Neto, J. C. Acquadro, P. R. Pascholati, E. Crema, C. Tenreiro, N. Carlin Filho, and M. M. Coimbra, Nucl. Phys. **A534**, 429 (1991).

[9] C. Muri, R. M. Anjos, R. Cabezas, P. R. S. Gomes, S. B. Moraes, A. M. M. Maciel, G. M. Santos, C. Tenreiro, R. Liguori Neto, J. C. Acquadro, P. A. B. Freitas, and J. Lubian, Eur. Phys. J. A **1**, 143 (1998).

[10] P. R. S. Gomes, T. J. P. Penna, R. Liguori Neto, J. C. Ac-

quadro, C. Tenreiro, E. Crema, N. Carlin Filho, and M. M. Coimbra, Nucl. Instrum. Methods Phys. Res. A **280**, 395 (1989).
[11] J. C. Acquadro, R. Liguori Neto, N. Carlin Filho, M. M. Coimbra, E. F. Chagas, and P. R. S. Gomes, Rev. Fis. Apl. Instrum. **4**, 352 (1986).
[12] R. Liguori Neto, J. C. Acquadro, P. R. S. Gomes, A. S. Toledo, E. Crema, C. Tenreiro, N. Carlin, M. M. Carlin, and M. M. Coimbra, Nucl. Phys. **A512**, 333 (1990).
[13] S. Cavallaro, L. Y. Xiao, M. L. Sperduto, and J. Delaunary, Nucl. Instrum. Methods Phys. Res. A **245**, 89 (1986).
[14] A. Gavron, Phys. Rev. C **21**, 230 (1980).
[15] L. C. Vaz, J. M. Alexander, and G. R. Satchler, Phys. Rep., Phys. Lett. **69**, 374 (1981).
[16] H. J. Krappe, K. Mohring, M. C. Nemes, and H. Rosser, Z. Phys. A **314**, 231 (1983).
[17] D. E. Di Gregorio, J. O. Fernandez Niello, A. J. Pacheco, D. Abriola, S. Gil, A. O. Macchiavelli, J. E. Testoni, P. R. Pascholati, V. R. Vanin, R. Liguori Neto, N. Carlin Filho, M. M. Coimbra, P. R. S. Gomes, and R. G. Stokstad, Phys. Lett. B **176**, 322 (1986).
[18] D. E. Di Gregorio, M. Di Tada, D. Abriola, M. Elgue, A. Etchegoyen, J. O. Fernandez Niello, A. J. Pacheco, A. M. Ferrero, S. Gil, A. O. Macchiavelli, J. E. Testoni, P. R. S. Gomes, V. R. Vanin, R. Liguori Neto, E. Crema, and R. G. Stokstad, Phys. Rev. C **39**, 516 (1989).
[19] N. Keeley, S. J. Benret, N. M. Clarke, B. R. Fulton, and G. Tungate, Nucl. Phys. **A571**, 326 (1994).
[20] A. M. M. Maciel, P. R. S. Gomes, J. Lubian, R. M. Anjos, R. Cabezas, S. B. Moraes, C. Muri, M. M. Sant'Anna, G. M. Santos, R. Liguori Neto, N. Added, N. Carlin, and C. Tenreiro, Phys. Rev. C **59**, 2103 (1999).
[21] G. R. Satchler, Phys. Rep. **199**, 147 (1991).
[22] M. A. Nagarajan, C. C. Mahaux, and G. R. Satchler, Phys. Rev. Lett. **54**, 1136 (1985).
[23] Y. Sakuragi, M. Yahiro, and M. Kamimura, Prog. Theor. Phys. **70**, 1047 (1983).
[24] Y. Sakuragi, M. Yahiro, and M. Kamimura, Prog. Theor. Phys. Suppl. **89**, 136 (1986).
[25] J. Raynal, in *Proceedings of the Workshop on Applied Nuclear Theory and Model Calculations for Nuclear Technology Applications, Trieste, 1988* (World Scientific, Singapore, 1988), p. 506.
[26] G. H. Rawitscher, Phys. Rev. C **9**, 2210 (1974).
[27] J. P. Farrel, Jr., C. M. Vincent, and N. Auster, Ann. Phys. (N.Y.) **96**, 33 (1976).
[28] M. Yahiro and M. Kamimura, Prog. Theor. Phys. **65**, 2046 (1981); **65**, 2051 (1981).
[29] N. Keeley and K. Rusek, Phys. Rev. C **56**, 3421 (1997).
[30] P. E. Hodgson, *Nuclear Reactions and Nuclear Structure*, edited by W. Marshall and D. H. Wilkinson (Clarendon, Oxford, 1971).
[31] M. E. Brandan, J. R. Alfaro, A. Menchaca-Rocha, J. Gomez del Campo, G. R. Satchler, P. H. Stelson, H. T. Kim, and D. Shapira, Phys. Rev. C **48**, 1147 (1993).